Juni Khyat ISSN: 2278-4632
(UGC Care Group I Listed Journal) Vol-10 Issue-6 No. 1 June 2020

An Approach For Dehazing Of Underwater Image By Using Multi-Scale Fusion Strategy

Jyothsna Pokanati
Lendi Institute of Engineering and Technology, Dept. of ECE
JNTU Kakinada, Vizianagaram, Andhra Pradesh, India

Sravani Tankala
Lendi Institute of Engineering and Technology, Dept. of ECE
JNTU Kakinada, Vizianagaram, Andhra Pradesh, India

Khan Sheik
Lendi Institute of Engineering and Technology, Dept. of ECE
JNTU Kakinada, Vizianagaram, Andhra Pradesh, India

Dileep Raghumajji
Lendi Institute of Engineering and Technology, Dept. of ECE
JNTU Kakinada, Vizianagaram, Andhra Pradesh, India

Ch. Gayatri M.Tech, MIE
Assistatnt Professor
Lendi Institute of Engineering and Technology, Dept. of ECE
JNTU Kakinada, Vizianagaram, Andhra Pradesh, India

Abstract— We introduce an effective technique to enhance the image captured underwater which are degraded medium due to scattering and absorption. Our method is based on multi-scale fusion strategy. In this method the original degraded image will be color compensated using white-balancing technique .This color compensated image will undergo gamma correction and sharpening. These two images will be fusioned using this multi scale fusion technique. Here we are getting better exposedness of dark regions; global contrast and edge sharpness of the image are improved. It is done using MATLAB code.

INTRODUCTION:

The underwater environment refers to the region below the surface and immersed in liquid water in a natural or artificial feature such as an ocean, sea, lake or canal. Unlike normal images underwater images suffer from poor visibility mainly due to two reasons. The main reason is absorption and scattering effects. The absorption reduces the light energy and scattering causes change in light propagation direction [1]. These result in appearance of fog and halo artifacts on the image which makes the visual quality of an image degraded. In common sea water images if the object to be captured is at more than 10 meters, it appears to be difficult to perceive and the colors appear to be faded. It becomes more challenging for image processors when only a single image is available. Solutions for such type of problems have been only introduced recently [7],[12]-[15]. The processing of underwater images focuses solely on compensating either light scattering or color change distortion. There are several enhancement techniques available in order to improve the visual quality of an degraded image such as exploitating the polarization effects to compensate for visibility degradation [10], using image dehazing to restore the clarity of underwater images [11], combining point spread functions and a modulation transfer function to reduce the blurring effect [27]. Although the above mentioned techniques can enhance scene contrast and increase visibility, there will be distortion due to wavelength attenuation.

In this paper we are providing a new technique which is a single image approach. In this method the original degraded image will be color compensated using white balancing method. The color compensated image undergo gamma correction and edge sharpening. The two images will be fusioned in order to get a clear output image. Our method is based on the principle of image fusion, a well-studied topic of computational imaging that has found many useful applications such as interactive photo montage [16], image editing [17], image compositing [18] [19] and HDR imaging [20] [21].The main idea is to combine several images into single one, retaining only the most significant features. Our technique has been tested extensively for a large set of different degraded images. Results on a variety of hazy images demonstrate the effectiveness of our fusion based technique.

Existing techniques:

The existing underwater dehazing techniques is categorized into several classes. The first class corresponds to the methods using specialized hardware. The divergent-beam underwater lidar imaging system uses an optical/laser –sensing technique to capture turbid underwater images. But these complex acquisition systems are costly and their power consumption is very high.

The second class consists of polarization based methods. These methods use a number of images of the same scene captured with different degrees of polarization. Polarization techniques are effective in recovering distant regions, but the limitation is it is not applicable to video acquisition. So these are used only with the scenes which are not constant.

The third class consists of approaches which uses multiple images in their processing. By changing the intensities of scene points under different weather conditions the depth discontinuities of the scene are detected. Deep photo system restore image by using the georeferenced digital terrain and urban 3D models. This is impractical to use as the additional information is not available.

In the fourth class it develops the similarities between light propagation in fog and underwater. There several single image dehazing techniques to restore images of outdoor foggy scenes. These dehazing techniques used to reconstruct the intrinsic brightness of objects by inverting the koschmieder's visibility model [29]. The underwater imaging is more challenging due to the fact that the degraded quality of the captured image is due to the scattering which depends on the light wavelength.

Recently many algorithms for underwater images which depends on dark channel prior(DCP) are introduced. The DCP is first introduced for outdoor scenes dehazing. In the underwater images, the method of chiang and chen divides the foreground and the background regions based on DCP and uses this data to remove the haze and color variations based on color compensation.

Fusion Based Technique:

In practice, there is no enhancing method that remove the haze effects of such degraded inputs completely. Therefore, taking into consideration the difficulties stated before, we process only one captured image of the scene, the algorithm generates the original image only two inputs that gets back color and visibility of the entire image.

Inputs:

By taking into consideration the previous dehazing approaches such as Tan [12], Tarel and Hautiere [15] and he et al [13], we searched for a standard technique that will properly while balance the original image. By white balancing the original hazy image we obtain our first input. By this step we aim to restore the natural color of the captured image, by eliminating unrealistic color casts that are caused by the atmospheric color.

In the previous years many white balancing methods [22]-[26] have been proposed in the literature (a systematic overview of the existing methods is presented in [27]). Many specialized techniques have been experimented in order to solve our problem. Since we aim for a computationally effective dehazing approach, we choose the shades-of-gray color constancy technique [25]. Besides of its simplicity, this low level approach of Finlayson and Trezzi [25] has shown to yield comparable results to those of more complex white balance algorithms. White balance algorithms identify the illuminant color and it's projections on RGB color channels. The main objective of white balance algorithms is to remove the unrealistic color casts of captured image and restore it's original color in order to improve the visible quality of degraded original image. The color compensated image's illuminance levels will be corrected using gamma correction. Each pixel in a image has brightness level, called luminance. This value is between 0 to 1, where 0 means complete darkness (black), and 1 is brightest (white).

Different camera or video recorder devices do not correctly capture luminance. Different display devices (monitor, phone screen, TV) do not display luminance correctly neither. So, one needs to correct them, therefore the gamma correction function. Gamma correction function is used to correct image's luminance.

A. The color compensated image is edge sharpened using a Gaussian filter. Human perception is highly sensitive to edges and fine details of an image, and since they are composed primarily by high frequency components, the visual quality of an image can be enormously degraded if the high frequencies are attenuated or completed removed. In contrast, enhancing the high-frequency components of an image leads to an improvement in the visual quality. Image sharpening refers to any enhancement technique that highlights edges and fine details in an image. The gamma corrected image and the edge sharpened image are fusioned in order to get dehazed clear output Image

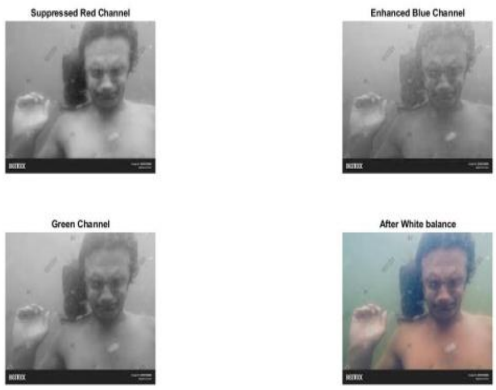

ISSN: 2278-4632
Vol-10 Issue-6 No. 1 June 2020


```
Noisy Image: nSig = 100.000, PSNR = 8.10

Iter = 1.000, PSNR = 12.53
Iter = 2.000, PSNR = 14.74
Iter = 3.000, PSNR = 17.58
Iter = 4.000, PSNR = 20.47
Iter = 5.000, PSNR = 21.93
Iter = 6.000, PSNR = 22.40
Iter = 7.000, PSNR = 22.61
Iter = 8.000, PSNR = 22.71
Iter = 9.000, PSNR = 22.79
Iter = 10.000, PSNR = 22.84
Iter = 11.000, PSNR = 22.88
Iter = 12.000, PSNR = 22.91
Iter = 13.000, PSNR = 22.93
Iter = 14.000, PSNR = 22.95
Estimated Image: nSig = 100.000, PSNR = 22.95
```

Multi-scale fusion:

Multi scale fusion process is a single image approach. Our underwater dehazing technique involves three steps. They are deriving input images from white balanced underwater image, definition of weight maps and multi scale fusion of inputs and weight maps.

Inputs of the fusion process:

As the color correction is difficult in underwater, we first apply our white balancing technique to the original Image. The main aim of this step is enhancing the image appearance by removing unwanted color casts caused by various sources.

In water deeper than 30 ft, white balancing suffers from some important effects since the absorbed colors are critical to be recovered. So, in order to get our ***first input*** we perform a gamma correction of the white balanced image version. Gamma correction aims at correcting the global contrast and is relevant. Since, in general white balanced underwater images tend to appear too bright. This correction increases the difference between darker/lighter regions at the cost of a loss of details in the under-/over-exposed region. To balance this loss, we derive a ***second input*** that involves a sharpened version of the white balanced image. Hence, we follow the unsharp masking principle, in the sense that we combine a blurred or unsharp (here Gaussian filtered) version of the image with the image to sharpen. The formula for unsharp masking defines the sharpened image S as

$$S = I + \beta(I - G * I)$$

where

I is the image to sharpen (in this case the white balanced image),

$G * I$ denotes the Gaussian filtered version of I,

and β is a parameter.

Practically the selection of β is not difficult. A small β fails to sharpen I, but a too large β results in over-saturated regions, with brighter highlights and darker shadows. To compensate this problem, the sharpened image S *is defined* as follows:

$$S = (I + N\{I - G * I\}) / 2$$

Where $N\{.\}$ denotes the linear normalization operator. This operator shifts and scales all the color pixel intensities of an image with the same shifting and scaling factor defined so that the set of transformed pixel values cover the entire available range.
The sharpening method defined has the advantage that it does not require any parameter tuning and sharpening appears to be efficient.
The second input helps to reduce the degradation caused by scattering. As the difference between white balanced image and its Gaussian filtered version is a high pass signal that approximates the opposite of Laplacian, this operation has the inconvenient to magnify the high frequency noise, thereby generating undesired artifacts in the second input. The multi-scale fusion strategy explained in the next section will reduce the transfer of those artifacts to the final fusioned image.

Weights of the Fusion Process

The weight maps are used during fusion in such a way that pixels with a high weight value are more shown in the final image. They are defined based on a number of local image quality or saliency metrics.
Laplacian contrast weight (W_L) predicts the global contrast by calculating the approximate value of a Laplacian filter applied on each input luminance channel. This indicator was used in many applications such as tone mapping and extending depth of field as high values are assigned to edges and texture. For underwater dehazing this weight is not applicable as it is not sufficient to recover the contrast, mainly because it cannot differentiate between a straight and flat regions. To solve this problem, we introduce other assessment weights.
Saliency weight (W_S) aims at enhancing the salient figures that lose their features in the underwater scene. To measure the saliency level, we have employed the saliency estimator of Achantay *et al.* [28]. This computationally effective algorithm has been inspired by the biological concept of center-surround contrast. However, the saliency map tends to help highlighted areas (regions with high luminance values). To avoid this disadvantage, we introduce an additional weight map based on the observation that saturation decreases in the highlighted regions.
Saturation weight (W_{Sat}) used in the fusion algorithm to adapt to chromatic information which is an advantage for highlighted regions. This weight map is simply calculated for each input I_k as the deviation (for every pixel location) between the R_k, G_k and B_k color channels and the luminance Lk of the *kth* input:

$$W_{Sat} = \text{sqrt}(1/3(R_k-L_k)2+(G_k-L_k)2+(B_k-L_k)2)$$

Generally for each input, the three weight maps can be combined in order to get a single weight map as follows. For each input k, an aggregated weight map W_k is first obtained by summing up the three W_L, W_S and W_{Sat} weight maps. The k aggregated maps are then reduced on a pixel-per-pixel basis, by dividing the weight of each pixel in each map by the sum of the weights of the same pixel over all maps. Note that, when compared with our previous work [30], we limit ourselves to these three weight maps only and we do not calculate the exposedness weight map anymore. By reducing the overall complexity of the fusion process, we observed that, if the two inputs proposed in the paper is used then the exposedness weight map amplifies some artifacts, such as ramp edges of our second input, and to reduce the benefit derived from the gamma corrected image in terms of image contrast. This observation can be explained as follows. Originally, in an exposure fusion context, the introduction of exposedness weight map is done to reduce the weight of pixels that are under-exposed or over-exposed. Hence, this weight map assigns large (small) weight to input pixels that are close to (far from) the middle of the image dynamic range. In this case, as the gamma corrected input tends to exploit the whole dynamic range, the use of the exposedness weight map tends to penalize it in favor of the sharpened image, there by inducing some sharpening artifacts and missing some contrast enhancements.

Naive Fusion Process:

If the normalized weight maps is given then the reconstructed image *R(x)* could typically be obtained by fusing the defined inputs with the weight measures at every pixel location *(x)*:

$$R(x) = \sum_{k=1}^{k} wk(x) Ik(x)$$

where I_k denotes the input (k is the index of the inputs k = 2 in our case) that is weighted by the normalized weight maps .W_k when practically applied the naive approach introduces undesirable halos. A prominent solution to overcome this limitation is to employ multi-scale linear or non-linear filters.

Multi-Scale Fusion Process:

The multi-scale decomposition is based on Laplacian pyramid which is described in Burt and Adelson [57]. The pyramid representation decomposes an image into a sum of bandpass images. The input image is filtered using each level of the pyramid using a low-pass Gaussian kernel G, and decimates the filtered image by a factor of 2 in both directions.
It then subtracts from the input an up-sampled version of thelow-pass image, thereby approximating the (inverse of the) Laplacian, and uses the decimated low-pass image as the input for the subsequent level of the pyramid. Using G_l to denote a sequence of l low-pass filtering and decimation, followed by l up-sampling operations, we define the N levels Ll of the pyramid as follows:

$I(x) = I(x) - G_1\{I(x)\} + G_1\{I(x)\}$ _ $L_1\{I(x)\} + G_1\{I(x)\}$

$= L_1\{I(x)\} + G_1\{I(x)\} - G_2\{I(x)\} + G_2\{I(x)\}$

$= L_1\{I(x)\} + L_2\{I(x)\} + G_2\{I(x)\}$

$= \ldots$

$= \sum_{i=1}^{N} Ll\{I(x)\}$

In this equation, L_l and G_l represent the *lth* level of the Laplacian and Gaussian pyramid, respectively. In order to write the equation, all those images have been up-sampled to the original image dimension. In an efficient implementation, each level *l* of the pyramid is manipulated at native subsampled resolution. By following the traditional multi-scale fusion strategy [55], each source input I_k is decomposed into a Laplacian pyramid [57] while the normalized weight maps. W_k are decomposed using a Gaussian pyramid. Both Laplacian and Gaussian pyramids have the same number of levels and the mixing of the Laplacian inputs with the Gaussian normalized weights is performed independently at each level l:

$$R(x) = \sum_{k=1}^{k} G\{W(x)\}L(I(x)\}$$

where *l* denotes the pyramid levels and *k* indicates the number of input images. In practice, the number of levels *N* depends on the image size, and has a direct effect on the visual quality of the fusioned image. The final dehazed output is obtained by adding the fused contribution of all levels, after appropriate upsampling. By independently applying a fusion process at every scale level, the potential artifacts due to the sharp transitions of the weight maps are minimized. Multi-scale fusion is motivated by the human visual system, which is very sensitive to sharp transitions appearing in smooth image patterns, while being much less sensitive to variations/artifacts occurring on edges and textures (masking phenomenon). A recent work has shown that the multiscale process can be approximated by a computationally efficient and visually pleasant single-scale procedure. This single scale approximation should definitely be applied when complexity is an issue, as it also turns the multiresolution process into a spatially localized procedure.

Results:

As we performed multiscale fusion process by employing white balancing, gamma correction, sharpening and then multi scale fusion by employing weights, Laplacian pyramids and Gaussian pyramids we generally see the results and compare it with other existing dehazing process in terms of it's mean square value and psnr value.

In order to quantitatively assess and rate the algorithms, we calculate the mean squares error (MSE). The MSE of each result can be calculated by the following equation:

$$e = \sqrt{\frac{1}{3N} \sum_{c \in \{r,g,b\}} \|\mathbf{J}^c - \mathbf{G}^c\|^2}$$

where J is the dehazed image, G is the ground truth image, J_c represents a color channel of J, G_c represents a color channel of G, N is the number of pixels within the image G, and e is the MSE measuring the difference between the dehazed image J and the ground truth image G. Note that J and G have the same size since they are corresponding with the hazy image I. Given J and G, a low MSE represents that the dehazed result is satisfying while a high MSE means that the dehazing effect is not acceptable. By calculating the MSE of both He et al.'s method and our method, the value of MSE of our method is two times smaller than He et al.'s method. Therefore, from this we can say that our method is quantitatively better than other methods.

He et al.'s method:

Mean square value: : 477007.10

Psnr value: 19.25

Our proposed method:

Mean square value: 200144.28

Psnr value:22.95

Conclusion:

we have discussed an alternative approach to enhance underwater videos and images. Our strategy doesn't require any additional information other than a single input image. In our approach we have shown that our method enhances a large number of underwater images

with high accuracy, being able to recover important faded features and edges.

REFRENCES

[1] Codruta O. Ancuti , Cosmin Ancuti , Christophe De Vleeschouwer . and Philippe Bekaert, "Color Balance and Fusion for Underwater Image Enhancement".

[2] R. Schettini and S. Corchs, “Underwater image processing: state of the art of restoration image enhancement methods” EURASIP J. Adv. Signal Process.. vol. 2010, Dec. 2010 , Art. no. 746052.
[3] C. O. Ancuti and C. Ancuti, “Single image dehazing by multi-scale fusion.” IEEE Trans. Image Process., vol. 22. No. 8, pp. 3271-3282, Aug. 2013.
[4] J. Y. Chiang and Y.-C. Chen, “Underwater image enhancement by wavelength compensation and dehazing,” IEEE Trans. Image Process., vol. 21, no. 4, pp. 1756–1769, Apr. 2012
[5] P. Burt and T. Adelson, “The laplacian pyramid as a compact image code,” IEEE Trans. Commun., vol. COM-31, no. 4, pp. 532–540, Apr. 1983
[6] M. D. Kocak, F. R. Dalgleish, M. F. Caimi, and Y. Y. Schechner, “A focus on recent developments and trends in underwater imaging,” Marine Technol. Soc. J., vol. 42, no. 1, pp. 52–67, 2008.
[7]] R. Fattal, “Single image dehazing,” in Proc. ACM SIGGRAPH, Aug. 2008, Art. no. 72.
[8]] P. Drews, Jr., E. Nascimento, F. Moraes, S. Botelho, M. Campos, and R. Grande-Brazil, “Transmission estimation in underwater single images,” in Proc. IEEE ICCV, Dec. 2013, pp. 825–830.
[9]] P. Drews, Jr., E. Nascimento, F. Moraes, S. Botelho, M. Campos, and R. Grande-Brazil, “Transmission estimation in underwater single images,” in Proc. IEEE ICCV, Dec. 2013, pp. 825–830.
[10] Y. Y. Schechner, N. Karpel, "Recovery of underwater visibility and structure by polarization analysis", *IEEE J. Ocean. Eng.*, vol. 30, no. 3, pp. 570-587, Jul. 2005.
[11] L. Chao, M. Wang, "Removal of water scattering", *Proc. Int. Conf. Comput. Eng. Technol.*, vol. 2, pp. 35-39, 2010.
[12] R. T. Tan, "Visibility in bad weather from a single image", *Proc. IEEE Conf. Comput. Vis. Pattern Recognit.*, pp. 1-8, Jun. 2008.
[13] K. He, J. Sun, X. Tang, "Single image haze removal using dark channel prior", *Proc. IEEE Conf. Comput. Vis. Pattern Recognit.*, pp. 1956-1963, Jun. 2009.
[14] L. Kratz, K. Nishino, "Factorizing scene albedo and depth from a single foggy image", *Proc. IEEE Int. Conf. Comput. Vis.*, pp. 1701-1708, Sep.-Oct. 2009.
[15] J.-P. Tarel, N. Hautiere, "Fast visibility restoration from a single color or gray level image", *Proc. IEEE Int. Conf. Comput. Vis.*, pp. 2201-2208, Sep.-Oct. 2009.
[16] A. Agarwala, M. Dontcheva, M. Agrawala, S. M. Drucker, A. Colburn, B. Curless, D. Salesin, M. F. Cohen, "Interactive digital photomontage", *ACM Trans. Graph. SIGGRAPH*, vol. 23, no. 3, pp. 294-302, 2004.
[17] P. Perez, M. Gangnet, A. Blake, "Poisson image editing", *ACM Trans. Graph. SIGGRAPH*, vol. 22, no. 3, pp. 313-318, 2003.
[18] R. Brinkmann, The Art and Science of Digital Compositing, San Mateo, CA, USA:Morgan Kaufmann, 1999.
[19] M. Grundland, R. Vohra, G. P. Williams, N. A. Dodgson, "Cross dissolve without cross fade: Preserving contrast color and salience in image compositing", *Comput. Graph. Forum*, vol. 25, no. 3, pp. 577-586, 2006.
[20] P. J. Burt, K. Hanna, R. J. Kolczynski, "Enhanced image capture through fusion", *Proc. IEEE Int. Conf. Comput. Vis.*, pp. 173-182, May 1993.
[21] T. Mertens, J. Kautz, F. V. Reeth, "Exposure fusion: A simple and practical alternative to high dynamic range photography", *Comput. Graph. Forum*, vol. 28, no. 1, pp. 161-171, 2009.
[22] G. Buchsbaum, "A spatial processor model for object colour perception", *J. Franklin Inst.*, vol. 310, no. 1, pp. 1-26, 1980.
[23] E. Land, J. McCann, "Lightness and retinex theory", *J. Opt. Soc. Amer. A*, vol. 61, no. 1, pp. 1-11, 1971.
[24] V. Cardei, B. Funt, K. Barnard, "Estimating the scene illumination chromaticity by using a neural network", *J. Opt. Soc. Amer. A*, vol. 19, no. 12, pp. 2374-2386, 2002.
[25] G. Finlayson, E. Trezzi, "Shades of gray and colour constancy", *Proc. 12th Color Imag. Conf.*, pp. 37-41, 2004.
[26] J. van de Weijer, T. Gevers, A. Gijsenij, "Edge-based color constancy", *IEEE Trans. Image Process.*, vol. 16, no. 9, pp. 2207-2214, Sep. 2007.
[27] W. Hou, D. J. Gray, A. D. Weidemann, G. R. Fournier, and J. L. Forand, “Automated underwater image restoration and retrieval of related optical properties,” in Proc. IGARSS, 2007, vol. 1, pp. 1889–1892.
[28] R. Achantay, S. Hemamiz, F. Estraday, and S. Susstrunk, “Frequency tuned salient region detection,” in *Proc. IEEE CVPR*, Jun. 2009, pp. 1597–1604.
[29] H. Koschmieder, “Theorie der horizontalen sichtweite,” *Beitrage Phys.Freien Atmos.*, vol. 12, pp. 171–181, 1924.
[30] C. Ancuti, C. O. Ancuti, T. Haber, and P. Bekaert, “Enhancing underwater images and videos by fusion,” in *Proc. IEEE CVPR*, Jun. 2012,pp. 81–88.

